Aquat Sci (2012) 74:735–750
DOI 10.1007/s00027-012-0257-4

Aquatic Sciences

RESEARCH ARTICLE

Spatial variability in sedimentation rates and artificial radionuclide storage in alluvial banks of the lower Rhône River

M. Provansal · E. Ferrand · F. Eyrolle · G. Raccasi · M. Monaco · R. Gurriaran

Received: 4 February 2011 / Accepted: 2 March 2012 / Published online: 17 March 2012

Abstract This paper analyzes the relationship between bank sediment storage and radionuclide content in six alluvial sites located in different geomorphic contexts along the lower Rhône River. The ^{137}Cs, ^{238}Pu, $^{239+240}$Pu, ^{241}Am and ^{210}Pb profiles show different patterns, which indicates a differential storage of contaminated sediment in the banks. Three sites record historical nuclear releases in the river and give evidence for long-term retention of particle-reactive long-lived radionuclides. Two sites record only atmospheric global fallout. Only one site, connected to the river groundwater, provides some evidence for desorption of particle-bound contaminants, with a low and constant ^{137}Cs activity profile. The history of the releases from the Marcoule spent-fuel reprocessing plant—the main source of artificial radioactivity—provides a reliable chronology of the last 50 years. Sediment grain size and bank topography are important factors in determining where artificial radionuclides are stored, but these two parameters cannot be used alone to determine variations in high concentrations of radionuclides. The chronology of fluvial geomorphic "metamorphosis" during the twentieth Century, especially after 1960, is also a critical factor affecting the spatial variability in sedimentation rates and artificial radionuclide storage; the timing of channel deepening and bank sedimentary accretion interfere with the chronology of major floods and the short period of low discharge during the height of contamination from nuclear liquid effluents. The reach-scale adjustment described in this paper can contribute to determining what the local history may have been. This result has important implications for river management decisions.

Keywords Fluvial geomorphology · ^{137}Cs · Plutonium · Riverbanks · Sedimentation · Floods · Rhône River

M. Provansal (✉) · G. Raccasi · M. Monaco
Aix-Marseille Univ, CEREGE, UMR 7330,
13545 Aix en Provence, France
e-mail: provansal@cerege.fr

F. Eyrolle
IRSN, Institut de Radioprotection et de Sûreté Nucléaire,
DEI/SESURE/LERCM, 13115 Saint Paul Lez Durance, France

E. Ferrand · R. Gurriaran
IRSN, Institut de Radioprotection et de Sûreté Nucléaire,
DEI/SESURE/LMRE, 91400 Orsay, France

Introduction

Sedimentation processes and accumulation rates in river alluvial margins have been examined in numerous studies (Steiger et al. 2003; Alekseevsky et al. 2008), several of which used isotopic analysis to date deposits and quantify sedimentation rates on the banks and alluvial plain (Collins et al. 1997; Walling and He 1997, 1998; Eyrolle et al. 2006; Piégay et al. 2008; Detriché et al. 2010). Due to the strong affinity of most elements for particle-reactive components (Hochella and White 1990; Middelkoop 2000), the spatial distribution of trace elements mainly depends on the nature or content of the finest constituents, i.e. clay, Fe and Mn oxyhydroxides, and organic matter. The grain size and deposit thickness of sediments are also widely considered to be major parameters in pollutant concentration and storage (Eyrolle et al. 2006; Detriché et al. 2010). Walling and He (1997) report positive correlations between ^{137}Cs content and the distance from the channel because the finest particles found in the farthest away from the channel display the highest concentrations overall.

Preliminary studies in the lower Rhône River have demonstrated the presence of artificial radionuclides in

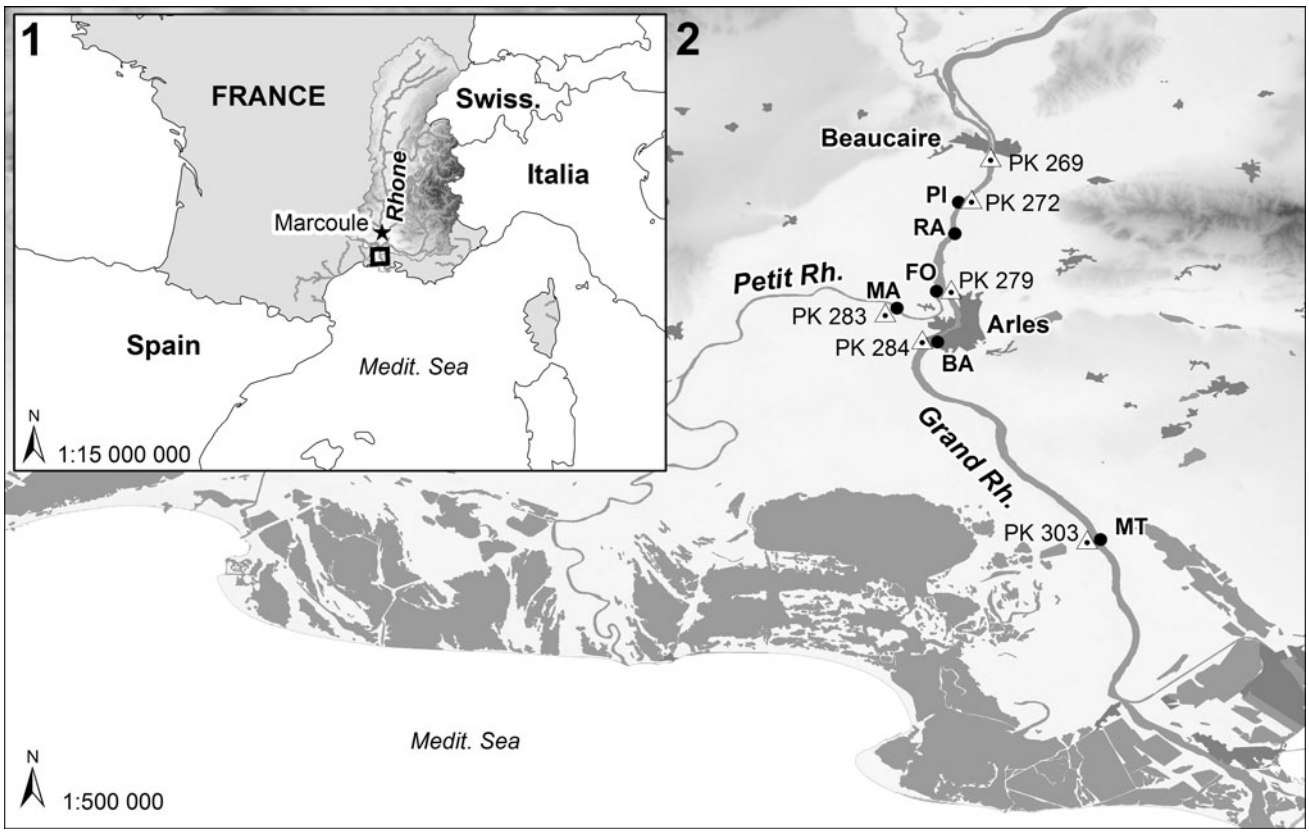

Fig. 1 Location of the lower Rhône River and the sampling sites

various sectors of the fluvial margins (Rolland 2006; Eyrolle et al. 2008a; Provansal et al. 2010; Ferrand et al. 2012) and in the Camargue delta (Miralles et al. 2006). The study area in the lower Rhône River is indeed located 70 km downstream of the Marcoule spent-fuel reprocessing plant (PK 210,[1] Fig. 1); i.e. the southernmost point of industrial radioactive releases, which was the main source of artificial radioactivity in the river over many years (Eyrolle et al. 2005). A good correlation was observed locally between the chronology of the deposits and radionuclide inputs released by the Marcoule plant (Provansal et al. 2010).

Several studies have highlighted the geomorphic changes in the fluvial system over the last century (Arnaud-Fassetta 2003; Antonelli et al. 2004; Raccasi 2008). Following fluvial management dating back to the end of the nineteenth Century, channel adjustments have resulted in heterogeneous fluvial "metamorphosis". As shown in other channelized fluvial systems (Surian and Rinaldi 2003; Kiss et al. 2008; Ciszewski and Turner 2009), local changes in sediment storage induced by river management could have influenced the spatial distribution of contaminants.

The aim of this study is to broaden previous local measurements (Provansal et al. 2010), to summarize geomorphological observations from various unpublished master's and PhD studies, and to propose an outline for the location of radionuclide sediment storage in a large managed and nuclearized river. The collaboration between geomorphologists and geochemists will help answer the following questions: how does fluvial geomorphology affect radionuclide storage in the margin sediments? What are the main factors controlling the heterogeneity of contaminant concentrations? Using this framework, we aim at a better understanding of the distribution of radioactive elements in the fluvial margin system that constitute a significant source of contaminated particles, and at contributing towards an appropriate global management policy of the riverbanks.

Regional setting, study sites

The lower Rhône: background characteristics and recent evolution

The study reach is located in the downstream part of the Rhône catchment (area: 98,000 km^2), on the wide base-level plain between Beaucaire and the Mediterranean Sea (Fig. 1). The mean 1920–2007 annual discharge at the

[1] PK: PK, for Kilometric Point: distance in km from the centre of the city of Lyon, the topographic reference used for the Rhône catchment.

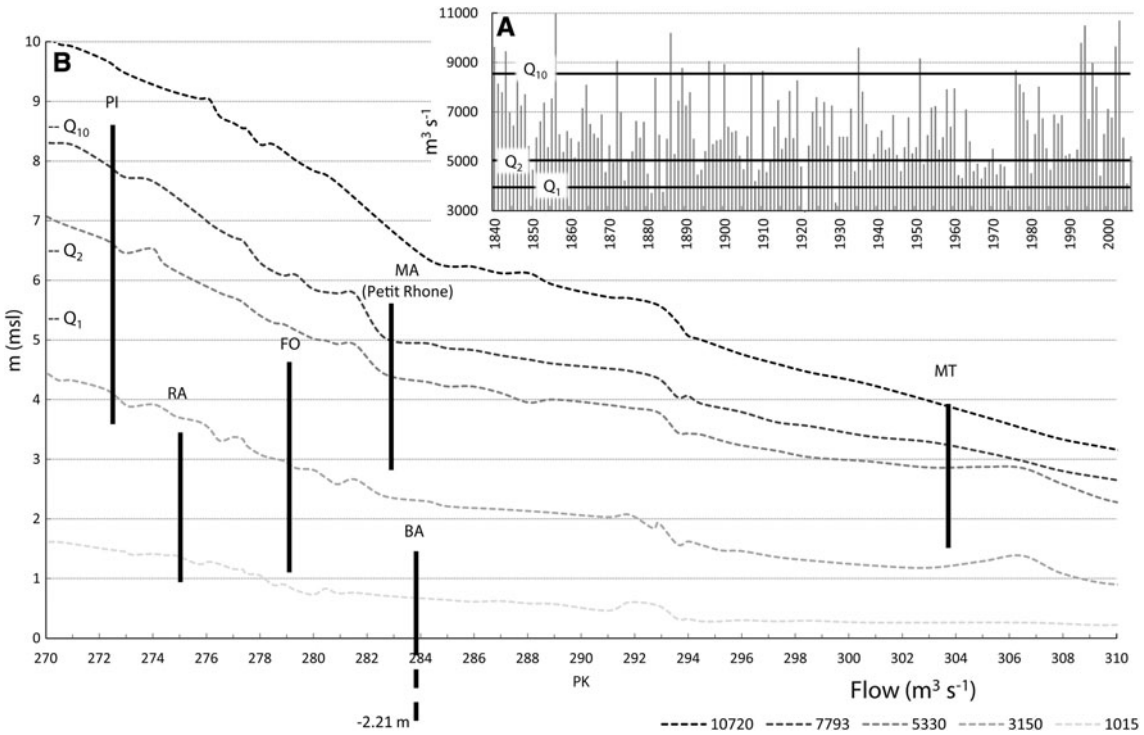

Fig. 2 **a** Highest annual Rhône River discharges from 1840 to 2007. **b** Water levels in the channel. The *vertical lines* show the position and height of the cores and the PI section (*left*, values of Q_1, Q_2, Q_{10} in the Beaucaire gauge station)

Beaucaire station is 1,720 $m^3 s^{-1}$. Several major floods occurred in the first decades of the twentieth Century, followed by a low-flow period, with moderate floods from 1940 to 1970. Typically, large floods—above Q_{10} discharge 8,000 $m^3 s^{-1}$—show an irregular chronological distribution, occurring more regularly over the last 15 years (Fig. 2a). The 10,500 $m^3 s^{-1}$ flood in December 2003 exceeded the 100-year return discharge. Upstream of the Camargue Delta, the Rhône River splits into two branches: the "Grand Rhône" (90 % of the discharge) and the "Petit Rhône" (10 % of the flux).

The mean annual Total Suspended Solid (TSS) flux is estimated at 6.7×10^6 tons at Arles (Pont et al. 2002). The drastic decrease (Fig. 2b) in longitudinal bed profile and water surface slopes (average 0.04 m km^{-1} between Beaucaire and the deltaic bifurcation 0.003 m km^{-1} in the Grand and Petit Rhône branches) causes a drop in stream power and enhances the sedimentation rate along the alluvial margins (Bravard 2010).

The engineering works built since the end of the nineteenth Century (non-floodable embankments, groynes, compartments[2] and barred arms, and subsequently hydroelectric dams) trapped sediments and induced a fluvial "metamorphosis" from a braided style to a sinuous one. Responses include simplification of channel morphology, erosion of the channel bed, bank-line mobility and infill of the alluvial margin, with significant differences in the location, chronology, thickness and grain size of the deposits (Antonelli 2002; Arnaud-Fassetta 2003; Antonelli et al. 2004; Raccasi 2008).

The fluvial system started to change at the beginning of the twentieth Century in the two deltaic branches (Fig. 3), as a result of the weaker energy slope and mobility of the sandy bed load (Antonelli 2002). The same process occurred later upstream, essentially during the second part of the twentieth Century, where it continues today. The sedimentary storage between 1876 and 2006 reached about 20×10^6 tons, specifically 6.3×10^6 tons along the Grand Rhône branch before 1950 and 12.8×10^6 tons in the Beaucaire-Arles plain after 1950 (Maillet et al. 2007). Moreover, the vertical erosion in the channel has progressively increased the capacity of the bed and reduced the flooding of high banks. Consequently, the grain size of the deposits is a function of bank topography: sandy-silt at the top of the high banks submerged only during high-energy Mediterranean events (50–100-year return period discharges), silt on the low banks flooded during 2–5-year return period discharges and silty-clay in former barred branches.

[2] Compartments: the usual technical French word is "casier", corresponding to crossed longitudinal and transverse dykes, which divide the borders of the main channel into several compartments. The system is different from the simple transverse dykes in the secondary barred arms.

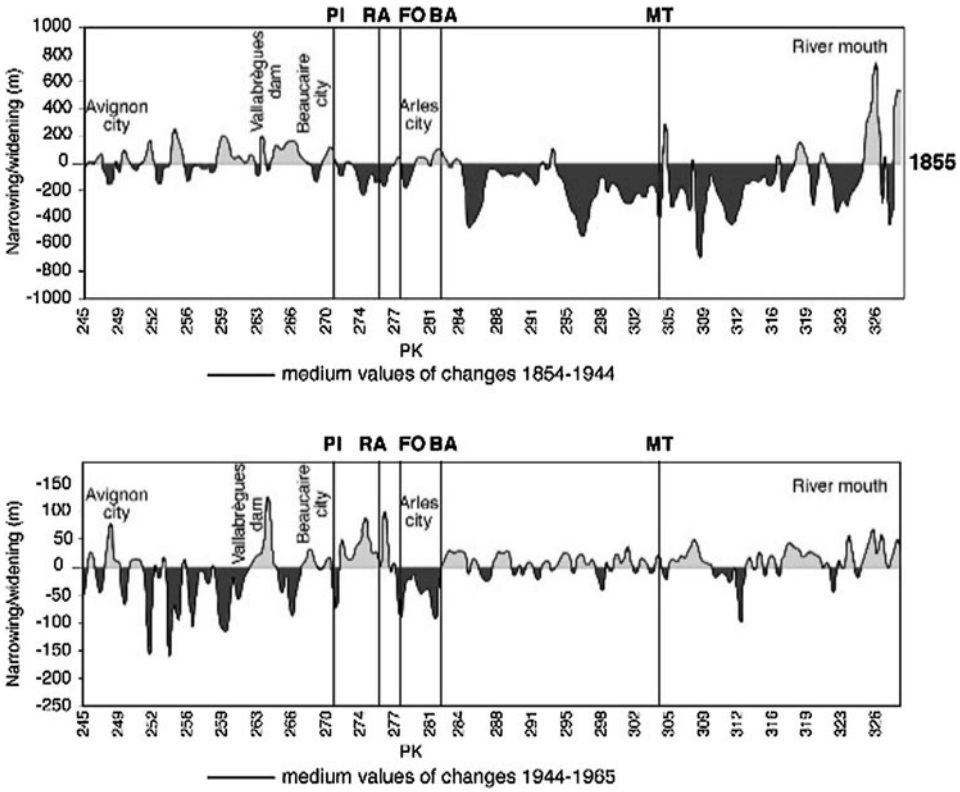

Fig. 3 Average values showing changes in channel width between 1855–1944 and 1944–1965. The locations of five study sites (without MA site) are shown by the *vertical lines* (based on Antonelli 2002). (1) Channel narrowing. (2) Channel widening

Study sites

Three sites are located upstream of the deltaic bifurcation (Fig. 4): PI (Pillet bank), FO (Fourques village) and RA (Ranchier), and three downstream (Fig. 5): BA (Barriol) and MT (Mas Thibert) on the Grand Rhône branch and MA (Mas de l'Aube) on the Petit Rhône branch. The six study sites are representative of the various environments that could influence the sedimentation rate and grain size of the deposits and their associated contaminant storage capacity in the lower Rhône River. They were selected on the basis of GIS diachronic analysis, field observations and the geomorphic classification established by Antonelli (2002) and Arnaud-Fassetta (2003). They were described using a total of 205 grain-size analyses (about 34 at each site) and 80 radionuclides analyses.

Three types of riverbanks and alluvial margins have been identified: high vertical banks, low gently sloping banks and former river branches. They differ in their morphology, relative height compared to water-flow (Fig. 2b), grain size and sedimentary chronology: high vertical banks (>3 m) have a specific stratigraphy, characterized by coarser deposits (sands or gravels inherited from the braiding period) at the base, then fine (silty) stratified deposits and silty sands at the top. These banks are either subject to erosion (PI site) or are fronted and stabilised by submersed dykes (MT and MA sites). Low (<3 m) gently sloping banks correspond to fine stratified clay-silty deposits. The shallow topography and various management works (fronted submersed dykes and compartments) enhance vertical accretion of fine sediments on these banks (FO and BA sites). In the various former branches cut off by submersible transverse dykes during the second part of the twentieth Century, weak currents are slowed by dense riparian forest in low humid areas close to the water-table level. These conditions favour fine-grained sedimentation and reduce re-suspension caused by erosion. The RA site is representative of this type of alluvial setting.

Vertical sedimentary accretion of the riverbanks only occurs during bankfull discharge (Q_{bf}) (Fig. 2a, b). Ra and BA sites are submerged at Q_1 flood levels, while FO is below at Q_2 flood level. Three floods reached or exceeded 8,000 $m^3\ s^{-1}$ (about Q_{10}) between 1976 and 1982: they flooded only the PI, FO, RA and BA sites. Seven large floods have occurred since 1993, each exceeding 8,500 $m^3\ s^{-1}$ ($>Q_{50}$), flowing over all the sites except MT. The $>Q_{100}$ flood in December 2003 flooded all the sites, including the MT site.

Materials and methods

Sediment sampling and analysis

At site PI, the sedimentary sequences were collected in 2006 from a natural cut bank (Provansal et al. 2010). At

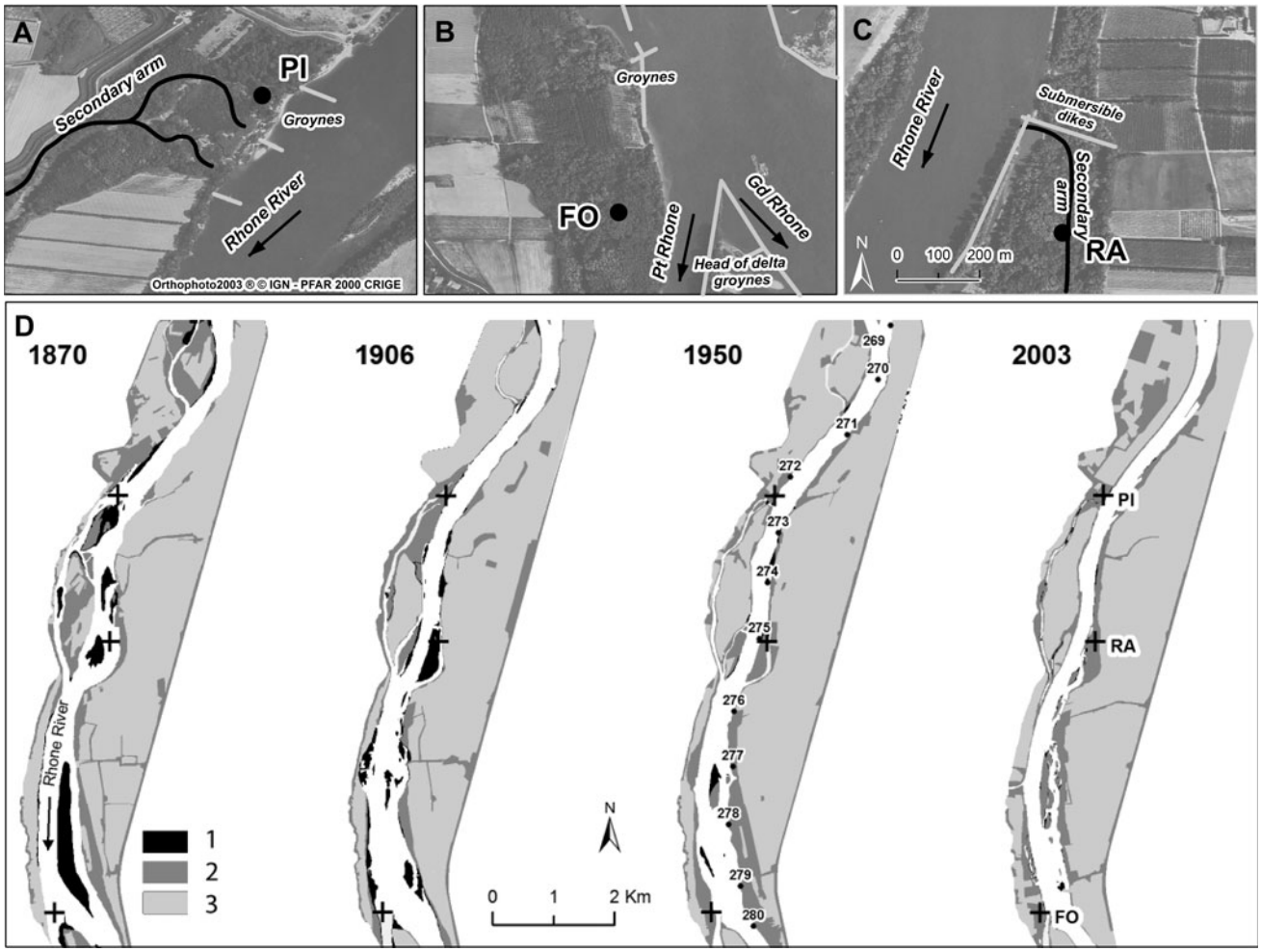

Fig. 4 Location (**a**, **b**, **c**); geomorphic evolution (**d**) of the sites PI, FO and RA since 1870. *1* Sandy or gravel banks, *2* afforested banks, *3* farming area

other sites, cores (0.08 m in diameter) were recovered above the average water-table level (1,015 m^3 s^{-1}). The total length is about 3 m at each site, except the RA site (1.2 m-long). All the core sites are located near the present main channel, except the RA core, which was extracted in a former branch. At sites FO and BA, the cores were extracted in two stages: the upper part in April 2003, before the December 2003 (Q_{100}) flood and the lower one in June 2004 after this event. The correlation between the two segments was established on the basis of the stratigraphic sequences, taking into account the thickness of the sandy layer deposited at the top by the 2003 flood.

Sediment samples were collected as a function of the main observed flood stratigraphic units (Reineck and Singh 1980; Provansal et al. 2010). Grain size was analyzed using the AFNOR X11-667 standards. A 10 g sub-sample was dried at 40 °C during 24 h and sieved at 2 mm to remove coarse organic debris and gravel. Organic matter was removed using 30 % hydrogen peroxide (Gee and Bauder 1986) and particle size measured by a Beckman-Coulter LS 230 laser particle-size analyzer. Duplicate sample analysis was performed on each sample to test the reproducibility of the procedure. Sediment textures were calculated by taking the average of the results obtained from each sub-sample. Sand, silt and clay fractions were defined as 2000-63, 63-2 and <2 μm, respectively.

Analyses of artificial and naturally occurring radionuclide

Around 80 g of selected fine-grained samples from stratigraphic units were freeze-dried, ground, sieved through a 2 mm mesh and conditioned into 60 ml containers. Gamma ray emitters from 200 samples were measured by direct gamma spectrometry with Germanium HP detectors (Bouisset and Calmet 1997). All detectable gamma emitters were quantified, as were excess ^{210}Pb ($^{210}Pb_{xs}$), by subtracting ^{214}Bi from total ^{210}Pb activity. The equilibrium between ^{226}Ra and ^{214}Bi was maintained by waiting at least a month after hermetically enclosing the sample in radon-

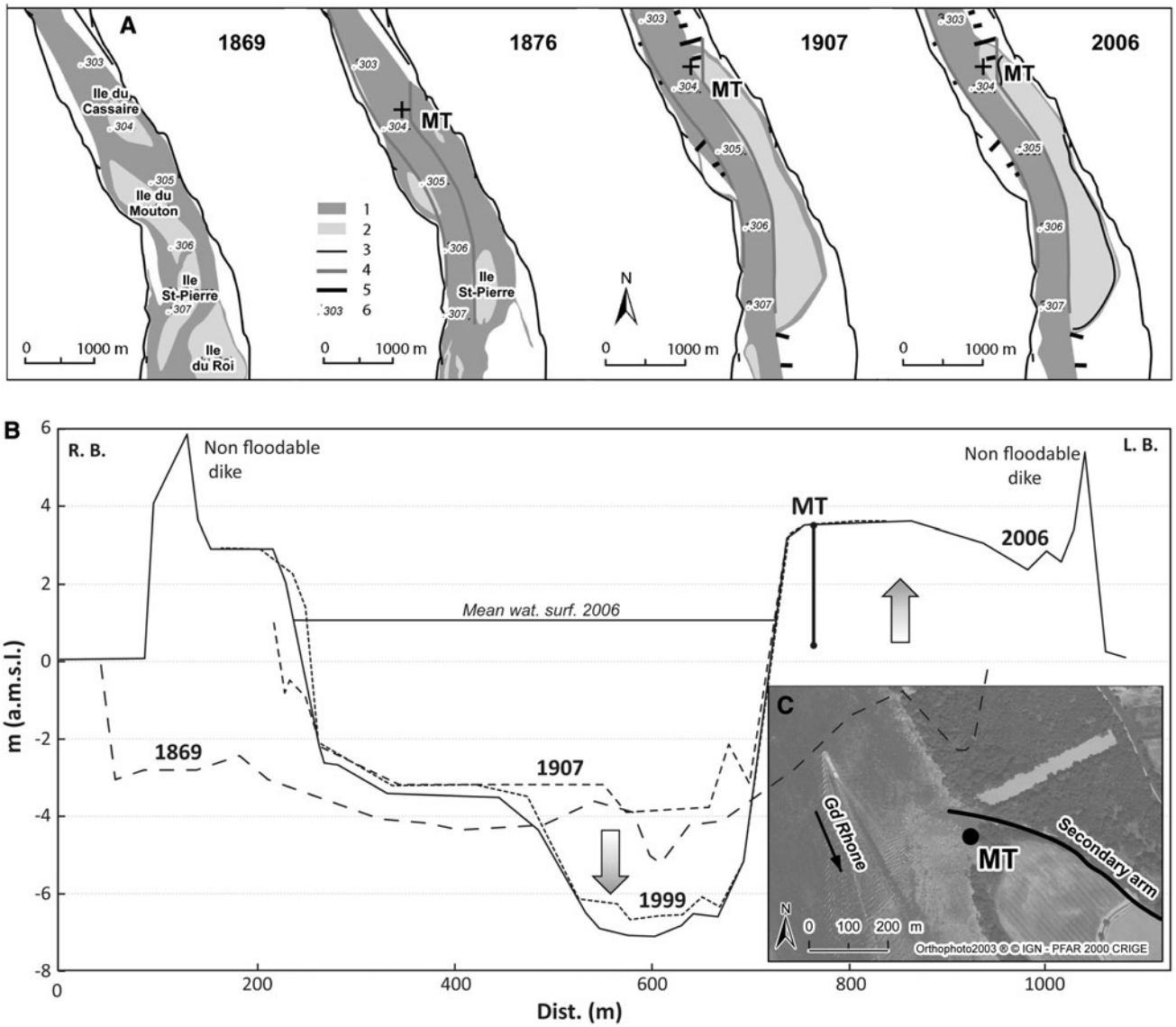

Fig. 5 Geomorphic evolution (**a**), evolution of the channel cross-sections (**b**), location and engineering woks (**c**) of the site MT. *1* Water area *2* sandy banks and *bars* *3* no floodable dykes *4* submersible dykes *5* groynes, *6* in front of the sites MT

tight containers. The low-energy gamma-emitting ^{210}Pb was measured after correcting for sample self-absorption (Bouisset et al. 1999). Measured activities, expressed as Bq kg^{-1} dry weight, were corrected for radioactive decay to the date of sampling. The activity uncertainty (at k = 2) is the combination of calibration uncertainties, counting statistics and summing self-absorption correction uncertainties. Plutonium isotopes, ^{238}Pu and $^{239+240}$Pu analyses were performed by alpha spectrometry on 33 samples from the PI, BA and MT sites, using the procedure described by Goutelard et al. (1998): samples were ashed (480 °C), spiked with ^{236}Pu to quantify the chemical yield, then leached with nitric acid, co-precipitated with $Fe(OH)_3$ and passed through exchangeable resins before being electrodeposited and counted on PIPS detectors for up to 14 days. ^{241}Am results were obtained either by gamma spectrometry or alpha spectrometry.

Chronological interpretation of the alluvial sedimentation/erosion budget

Maps, cross-sections and longitudinal profile surveys provide data on historical changes in channel and alluvial margin geometry since the late nineteenth Century (Antonelli et al. 2004; Raccasi 2008). The data sources were geographically referenced, corrected, and incorporated into a GIS database using Esri Arcview software, with an error margin between 5 and 10 m.

At sites PI, FO and RA, four maps dated between 1870 and 2003, as well two bathymetric surveys (1876 and 2006)

describe the 2D and 3D evolution since the end of the nineteenth Century (Fig. 4). At site PI, both dendrochronological data from a poplar tree and flood history indicate a nearly 5 m thick accumulation after 1970 (Provansal et al. 2010). At site MT (Fig. 5), four maps dated between 1869 and 2006, as well as four bathymetric surveys between 1907 and 2006, describe the 2D and 3D evolution since the end of the nineteenth Century. At site MA, the 3D evolution was analyzed using the1876 topo-bathymetric map and the 2002–2004 bathymetric survey. The link between the sedimentological records and hydraulic data over the last 20 years (1990–2009) has been established: the deposits of well-known major flood events were easily observed in situ.

Sediment dating and source term identification using radiotracers

^{210}Pb and ^{137}Cs are widely used for dating recent sediment deposits (less than 100 years) because of their respective half-lives of 22.3–30.2 years (Walling and He 1997; Piégay et al. 2008). Dating using $^{210}Pb_{xs}$ is commonly used for lake sediments where inputs of ^{210}Pb-bearing particles are continuous (Appleby et al. 1988). Although the method was shown to be less successful for riverbanks or floodplains largely due to a significant discontinuity and variability of deposition rates determined by flooding occurrence and magnitude, an average long-term sedimentation rate can sometimes be estimated (He and Walling 1996; Aalto and Dietrich 2005; Aalto et al. 2008).

Assuming that the atmospheric flux of ^{210}Pb is constant, the apparent sedimentation rate, V_{sed} can be estimated from the linear regression $\ln^{210}Pb_{xs}$ versus depth (z) by the following equations:

$$\ln^{210}Pb_{xs(z)} = az + \ln^{210}Pb_{xs(z=0)}$$

$$V_{sed}\left(cm \cdot year^{-1}\right) = -\lambda/a$$

a = the slope of the linear relationship and λ = the ^{210}Pb radioactive decay constant ($\lambda = 3.11 \times 10^{-2}$ year^{-1}).

In the specific case of the downstream part of the Rhône River, liquid releases of ^{137}Cs and other artificial radionuclides such as ^{241}Am and plutonium isotopes from the Marcoule spent-fuel reprocessing plant over recent decades (Fig. 6) are useful tools to estimate the approximate age of the various sedimentary sequences (see Provansal et al. 2010 for details).

Artificial radionuclides accumulate within accreting overbank sediment deposits in two ways: first by atmospheric fallout and second by deposition of suspended sediment (He and Walling 1996) that may have been contaminated by radionuclides from the nuclear fuel reprocessing facility. The changing ratios of artificial radionuclides, such as Pu isotopes, can help to identify these different source terms. Indeed, the data acquired for French river sediments upstream of any nuclear facility show an average ^{238}Pu/$^{239+240}$Pu activity ratio characteristic of the global atmospheric fallout of 0.036 ± 0.006 (Eyrolle et al. 2008b). In the lower Rhône valley, the Marcoule plant has generated radioactive liquid discharges including Pu since 1958 (Eyrolle et al. 2004). Between 1970 and 1998, the ratio increased from 0.05 to around 0.3 as a result of increased reprocessing of fuel from the nuclear electric power plants and decreased reprocessing of fuel of

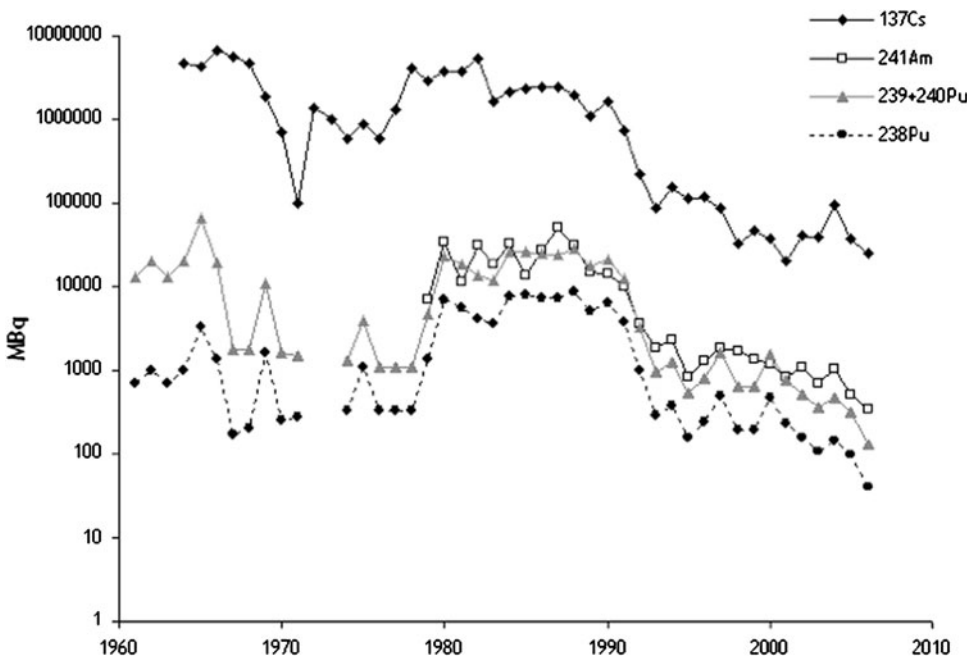

Fig. 6 Radionuclide source terms for Rhône River waters in MBq year^{-1} (10^9 Bq year^{-1}), since the first releases in 1954 (from Eyrolle et al. 2005)

military origin (Duffa and Renaud 2005). Furthermore, an activity ratio of 0.3 is the highest value recorded within the aquatic system downstream from the Marcoule plant over the past 40 years, whether in river bed sediments, bank accretion, aquatic mosses or suspended particles (Thomas 1997; Rolland et al. 2004; Eyrolle et al. 2008b). During the 2001–2008 survey (Eyrolle et al. 2008a), the Pu isotope activity ratio in the suspended load was highly variable, from 0.03 to 0.3, depending on the contribution of industrial liquid releases either from primary sources or secondary ones through re-uptake of contaminated sediments.

Results

Vertical variations in the grain-size and ^{137}Cs, ^{238}Pu, $^{239+240}$Pu, ^{241}Am and ^{210}Pb$_{xs}$ activity are shown in Fig. 7. Each vertical profile displays a location-specific pattern. ^{238}Pu and $^{239+240}$Pu activity as well as ^{238}Pu/$^{239+240}$Pu activity ratios are described in Table 1. Using the measured activity, the sites are separated into three groups (i) PI, FO and BA, (ii) MA and MT and (iii) RA.

Sites PI, FO and BA

These sites are characterized by relatively high or at least detectable concentrations of ^{137}Cs and ^{210}Pb$_{xs}$ along the profiles, which gives evidence for a progressive sediment accumulation.

Site PI (Figs. 4, 7; Table 1)

Site PI (PK 272.5) corresponds to a natural 9 m high section. Above the gravelly base linked to the braided fluvial system during the end of the nineteenth Century, grain-size variations in about 7 m of fine deposits show two types of depositional conditions: high-energy facies (silty sands) at the base and on the summit (60–70 % > 63 mm) and medium to low-energy facies (silts, fine silts, 60–70 % < 63 mm) in the middle part. In the top layer, sandy vertical accretion is very rapid, as a result of the large floods that occurred after 1990. The variability in grain size and the strong variations in sedimentation rates (Provansal et al. 2010) could explain the high variability in ^{210}Pb$_{xs}$ activity within the profile, which is not of use in dating the deposits.

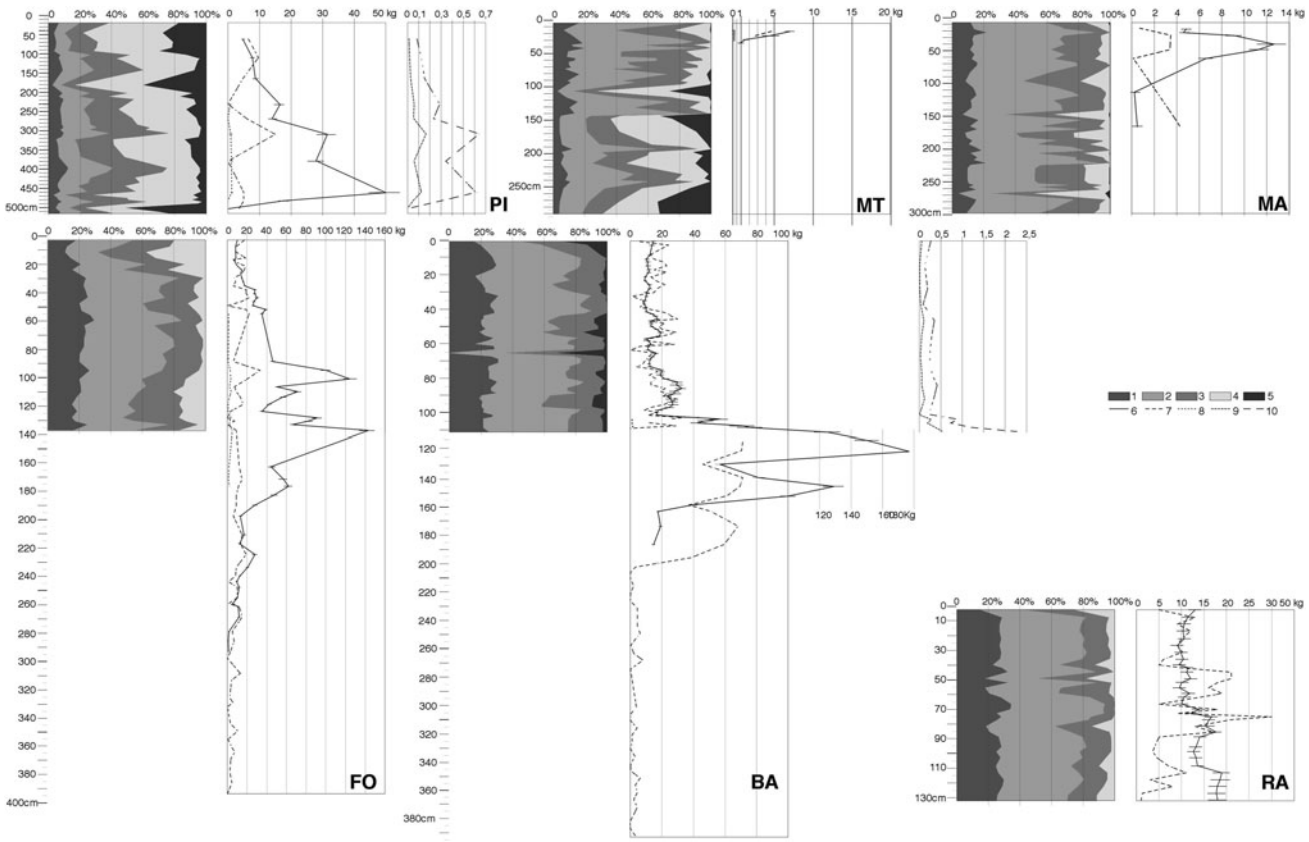

Fig. 7 Stratigraphy, grain size and radionuclide activity (in Bq kg^{-1}) at the six studied sites. Grain size: *1* clay (<2 mm), *2* fine silt (2–20 mm), *3* coarse silt (20–63 mm), *4* fine sand (63–250 mm), *5* medium and coarse sand (>250 mm). Radionuclide activity: *6* ^{137}Cs (with *error bars*), *7* ^{241}Am, *8* ^{210}Pb$_{xs}$, *9* ^{238}Pu, *10* $^{239+240}$Pu

Table 1 ^{238}Pu and $^{239+240}$Pu activity in mBq kg^{-1} and calculated ^{238}Pu/$^{239+240}$Pu activity ratios (AR Pu) in sites PI, MT and BA

Site	Depth (cm)	$^{239+240}$Pu	^{238}Pu	AR Pu
PI	40–83	86 ± 4	14 ± 1	0.16
	100–120	124 ± 6	19 ± 2	0.15
	120–210	153 ± 6	28 ± 2	0.19
	212–252	288 ± 10	59 ± 3	0.21
	252–288	235 ± 9	53 ± 3	0.23
	301–321	644 ± 21	166 ± 8	0.26
	351–409	346 ± 18	59 ± 6	0.17
	452–472	614 ± 23	122 ± 7	0.20
	478–488	314 ± 14	53 ± 5	0.17
	492–516	8 ± 1	0.8 ± 0.4	0.1
MT	10–21	244 ± 12	9.6 ± 1.6	0.04
	31–33	38 ± 4	1.7 ± 0.8	0.04
	56–60	1.6 ± 0.9	<1	–
	65–70	0.32 ± 0.34	<0.5	–
	75–87	1.9 ± 0.7	<0.6	–
	94–100	<0.5	<0.9	–
	119–124	<0.5	<0.6	–
	190–198	<0.5	<0.6	–
BA	0–3	263 ± 31	64 ± 15	0.24
	12–14	119 ± 20	11 ± 6	0.09
	24.5–26.5	181 ± 26	22 ± 9	0.12
	34–36	85 ± 18	38 ± 12	0.45
	44–45.5	344 ± 29	116 ± 16	0.34
	53.5–55.5	283 ± 30	53 ± 13	0.19
	65–66	231 ± 30	31 ± 11	0.14
	76–77	294 ± 21	60 ± 9	0.20
	82–83.5	411 ± 26	62 ± 10	0.15
	89.5–91	328 ± 41	121 ± 25	0.37
	99.5–100.5	205 ± 20	ND	–
	102–104	889 ± 48	282 ± 26	0.32
	105.5–108	722 ± 37	189 ± 18	0.26
	109–110	1208 ± 44	350 ± 22	0.29
	110–112	2267 ± 57	542 ± 24	0.24

The basal silty-sand units, characterized by ^{137}Cs activity (0.4 Bq kg^{-1}) influenced by the global atmospheric fallout after 1954 and by an AR Pu value (0.1) has been deposited after 1954, though it could be enriched in ^{137}Cs due to downward migration from the sandy overlying units (Forsberg et al. 2000; Miralles et al. 2004; Ciszewski et al. 2008). In the middle of the profile (4.8–2.1 m), both the presence of ^{241}Am and the significant increase in ^{137}Cs activity (50 Bq kg^{-1} at 4.5 m) correspond to the increasingly radioactive liquid effluents released by the Marcoule plant since the early 1960s (Fig. 6). According to growth rings at the base of a poplar tree trunk (Provansal et al. 2010), the deposits are dated between 1970 and 1972 at a 4 m depth. In the last 2.1 m, at the top of the bank, ^{137}Cs concentrations fall by a factor 5, then by a factor 10 and ^{241}Am activity falls below detection limits, corresponding to the decrease in ^{137}Cs and ^{241}Am releases from the reprocessing plant since 1990–1997 (Fig. 6). ^{238}Pu and $^{239+240}$Pu activity profiles, which first show an increasing then a decreasing trend, can also be linked to a change in Marcoule radioactive inputs. AR Pu varies from 0.17 to 0.26, then 0.16, suggesting a mixture of global fallout inputs and liquid discharges from Marcoule between the 1970s and the 1990s. Information obtained from various isotopes was therefore consistent and gave a reliable date for the middle part of the profile. These results reveal very high sedimentation rates during the second part of the twentieth Century, up from 0.04 cm year^{-1} in 1960–1972, a period with a very low frequency of large floods, to 13 cm year^{-1} in 1972–1990 (coinciding with the height of industrial radioactive activity) and then 30 cm year^{-1} from 1997 to 2003.

Site FO (Figs. 4, 7)

Site FO (PK 279.1) is located on a 2 m-high bank, protected by a submersible dyke and a compartment. In the 3.25 m long core, grain-size variations show three types of depositional conditions: sandy-silt layers (16–20 % > 63 mm) at the base, clayey silt (95–98 % < 63 mm) in the middle part, silty sands and sands (60–70 % > 63 mm, with sands >200 mm) at the top, which definitely correspond to deposits from flood events during the 1993–2002 decade.

Highly variable values in ^{210}Pb$_{xs}$ activity along the profile (Fig. 8) can be partly explained by the discontinuous sediment input. Using the mean of ^{210}Pb$_{xs}$ values at the top (18 Bq kg^{-1}) and at the bottom of the profile (2–4 Bq kg^{-1}), the overall age of the core could be estimated at between 30 to 50 years, corresponding to an apparent sedimentation rate of about 9.7 cm year^{-1}. ^{137}Cs and ^{241}Am provide additional data for the chronological interpretation of these sedimentary profiles.

^{137}Cs activity displays low but detectable levels in the base layers (around 0.5 Bq kg^{-1}), which have been deposited after 1954. From a depth of 200 cm, ^{137}Cs activity increases progressively then rapidly, associated with the detection of ^{241}Am. Two main peaks appear at 137 and 101 cm, with maximum values of 143 and 124 Bq kg^{-1}, respectively. In the last 70 cm, at the top of the bank, concentrations in ^{137}Cs fall to weaker values (from 28 Bq kg^{-1} at 58 cm to less than 10 Bq kg^{-1} in the upper layers) and ^{241}Am levels fall to below detection. This pattern illustrates the chronology of the release of radioactive waste from the Marcoule plant (Fig. 6).

These results reveal a very high sedimentation rate during the second part of the twentieth Century, varying from 16.5 cm year^{-1} in 1954–1960 to 2.5 cm year^{-1} in

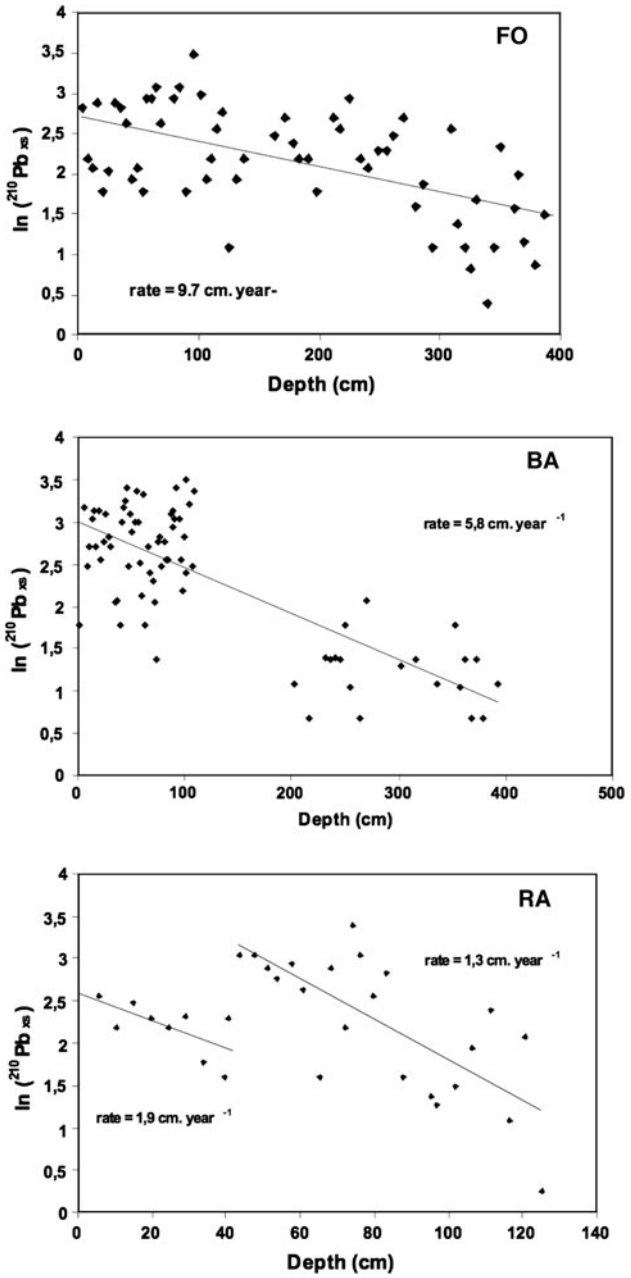

Fig. 8 Profile of $^{210}Pb_{xs}$ activity plotted on a log scale relative to depth at sites FO, BA and RA

1960–1990, coinciding with the height of industrial radiation activity, to 6.5 cm year^{-1} in 1990–1997 and 9.7 cm year^{-1} in 1997–2003. In the lower part, both the low altitude of the bank and trapping in the artificial compartments lead to an increase in the sedimentation rate. In the upper layers, ^{137}Cs activity profile gives the same apparent sedimentation rate as the $^{210}Pb_{xs}$ method, because the upper layers were more influenced by atmospheric inputs than fluvial ones. On average, the apparent sedimentation rate determined in site FO is very likely to be about 6–7 cm year^{-1} during the second part of the twentieth Century, comparable to those obtained in the previous site.

Site BA (Figs. 5, 7; Table 1)

This site (PK 284) is located on the 1.5 m high left bank at the entrance to the Barriol navigation lock (built in the early 1970s). In the 2.5 m long core, grain size, analyzed in the upper segment only, shows mainly clayey silt (95–98 % < 63 mm). At the top, the thick sandy silt layer (25–30 % > 63 mm) corresponds to deposits from flood events in the 1993-200 decade (Rolland 2006). The $^{210}Pb_{xs}$ activity varies along the profile (Fig. 8), but shows only low and thus very uncertain values: the rough apparent calculated sedimentation rate is 5.8 cm year^{-1}. The AR Pu ratio, only analyzed in the upper part, varies from 0.09 to 0.45. Two ^{137}Cs and ^{241}Am activity peaks, above 120 and 4 Bq kg^{-1} respectively, are identifiable at 145 and 120 cm. Their activity decreases below, but ^{137}Cs it is still detectable until 200 cm. From 100 cm to the top of the core, ^{241}Am disappears and ^{137}Cs decreases rapidly to 10–15 Bq kg^{-1}. As in the previous cores, these variations are interpreted as the result of the industrial chronology of the Marcoule plant (Fig. 6). On this basis, the upper part of the core, from the surface down to a depth of 40 cm, can be attributed to the 1997–2003 period (sedimentation rate 7 cm year^{-1}). The layers between 40 and 100 cm correspond to the 1990–1997 period (sedimentation rate 8.3 cm year^{-1}). Between 100 and 190 cm, ^{241}Am and ^{137}Cs activity is consistent with the chronology of the radioactive releases from Marcoule between 1960 and 1990 (sedimentation rate around 3 cm year^{-1}). Before this period, no ^{137}Cs activity was detected in the profile. As in site FO, the dating method using ^{137}Cs and $^{210}Pb_{xs}$ profiles indicates a globally high sedimentation rate, around 6 cm year^{-1}, during the second part of the twentieth century.

Sites MT and MA

Site MT (Figs. 5, 7; Table 1)

This site (PK 303) is located 15 km downstream of the deltaic bifurcation on a 3.5 m-high bank, protected by a submersible dyke. In the 3 m long core, grain-size variations show a sharp contrast between high-energy facies at the base (silty-sand and sandy layers—25–33 % > 200 µm coarse sand material—with low angle, then sub-horizontal laminations) and medium to low-energy facies in the upper part (clay and silty clay with 77–100 % < 63 µm, with horizontal laminations). This pattern reflects progressive construction of the bank, first by energetic processes near the channel, then by washload deposition at the top during floods. On the summit, a thick sandy layer (0.2 m),

disturbed by abundant organic debris, was deposited during the 2003 flood.

^{137}Cs is the only artificial gamma emitter measured above detection limits under the upper layer. Although the proportion of fine particles (<63 μm) is high, measured activity is weak (from 0.7 to 7 Bq kg^{-1}) and rapidly decreases with depth until a depth of 36 cm, where it falls under the limit of detection. In deeper areas, the ^{210}Pb$_{xs}$ profile is markedly similar to the ^{137}Cs profile.

These observations suggest there was atmospheric input on a rather stable alluvial surface, as described by Walling and He (1997) and Detriché et al. (2010). Furthermore, the calculated AR Pu ratio (0.04 in the two upper layers) are a typical signature of global atmospheric fallout, which would exclude the input of sediment released from the Marcoule plant and the weak sedimentation rate in this site in recent decades.

Site MA (Figs. 5, 7)

This site (PK 283) is located 2 km downstream of the deltaic bifurcation, on a 2 m-high bank under cultivation. In the 2.9 m long core, grain-size variations show low variability: silt and clay are predominant (80 % < 63 mm), except in four sandy-silt layers (25 % > 63 mm) in the lower part and at the top.

No significant ^{210}Pb$_{xs}$ was measured, which suggests that the deposits were not influenced by atmospheric inputs. ^{137}Cs is the only artificial gamma emitter measured above detection limits. In spite of a dominant silty-clay grain size, measured activity varies between 0.5 and 13 Bq kg^{-1}, with a peak at a depth of 40 cm. As in the MT site, ^{241}Am activity is undetectable and the values in the AR Pu ratio are very low. The low ^{137}Cs activity and the rapid decrease with depth suggest a rather stable alluvial surface, characterized by no major inputs from the nuclear plant and very weak sedimentation rates in recent decades.

Site RA (Figs. 4, 7)

The site (PK 274.5), representative of several humid alluvial patches, is located in a former branch. The 1.32 m long core was collected in the axis of the former branch (Rolland 2006). Grain size exhibits low variability, with mostly clayey silt (95–99 % < 63 μm). The 5 cm-sandy silt layer at the top (25 % > 63 μm) probably corresponds to deposits from the 2002 flood events that occurred before core sampling.

^{210}Pb$_{xs}$ exhibits low values (<30 Bq kg^{-1}), huge variations and a decreasing trend along the profile (Fig. 8). Applying the ^{210}Pb$_{xs}$ dating method, the apparent sedimentation rate is 1.9 cm year^{-1} in the upper 40 cm and 1.3 cm year^{-1} below. Therefore, the sediments would have been deposited over the last 90 years. However, these sedimentation rates are subject to strong uncertainties due to low ^{210}Pb$_{xs}$ activity. The ^{137}Cs profile is weak and homogeneous, ranging from 10 to 20 Bq kg^{-1}, without any significant trend with depth. It could indicate that the whole core has accumulated since the end of the 1990s, i.e. during a period of about 5 years (late 1997-early 2003), producing a large sedimentation rate (almost 26 cm year^{-1}). This chronological contradiction will be further discussed below.

To conclude, three successive types of sedimentary bedsets, covering a large range of particle grain sizes, characterize the study sites, except site RA: the coarsest deposits at the base (sites PI, FO, MA and MT), clayey-silty beds with a few sandy-silty interbeds in the middle part (sites PI, BA, MA) and a coarser sand layer at the top of all the sections. Coarse sediments at the base are correlated with deposits by bedload transport on the margin of a shallow braided channel; fine sediments in the middle part have been deposited by washload on the top of the forested bank; at the top, one or more coarser beds were deposited by the stronger Mediterranean floods of the last decade. Therefore, precise chronologic correlations between the different sections are impossible to determine.

^{137}Cs, ^{238}Pu, $^{239+240}$Pu and ^{241}Am activity profiles are different between the six study sites. Sites PI, FO and BA show significantly higher ^{137}Cs activity levels that those currently measured within suspended particles in the lower Rhône River (Antonelli et al. 2008; Eyrolle et al. 2008b). These sites also show detectable ^{241}Am, higher plutonium activity levels and ^{238}Pu/$^{239+240}$Pu activity ratios, close to those for liquid effluent reprocessing, at depths representing the historical radioactive releases by the Marcoule plant. These observations support the evidence of long-term retention of particle-reactive radionuclides within alluvial margins. In the deltaic MT and MA cores, ^{137}Cs activity is rather weak, rapidly decreasing from surface to depth and ^{241}Am was not detected. In the MT core, ^{238}Pu/$^{239+240}$Pu activity ratios are characteristic of atmospheric global fallout. This indicates a restricted accumulation of sediments over the last 50 years. At the top, the low ^{137}Cs and Pu activity in the deposits of the Q^{100} 2003 flood are probably the result of hysteretic cycles, which can lead to weak activity levels during the water retreat period after the flood peak. Site RA, which is regularly connected with the river groundwater, displays constant ^{137}Cs activity values along the profile. ^{210}Pb$_{xs}$ activity profiles differ significantly from site to site and are generally characterized by high variability along the core. This points to large disruptions in sedimentation processes and reveals the limits of this tool for quantifying sedimentation rates within alluvial margins.

Interpretation and discussion

Several factors could explain the variability of radionuclide trapping within alluvial margins of the lower Rhône River: the nature of the fluvial flux, the ways in which sediment was deposited (grain size, bank morphology), evolution following deposition, and geomorphological changes in the river system.

Relationship between liquid discharge, TSS flux and radionuclide concentrations

^{137}Cs activity within TSS flux is not correlated with liquid discharge. In 2007, without major flood events, ^{137}Cs activity measured in the washload was between 12.7 and 49.8 Bq kg^{-1}, in good correlation with the current output from the Marcoule and other nuclear plants located along the Rhône River. During the 2003 flood event, the ^{137}Cs activity in washload was 14.9 ± 0.4 Bq kg^{-1} (Antonelli et al. 2008). The same results are observed in sediment deposited by floods during the past 10 years at the top of the six study sections: the deposits associated with the 2003 flood show ^{137}Cs values below 10 Bq kg^{-1}.

The low activity measured on the top of MT and MA sections in sediments deposited by the 2003 flood, could, however, be explained by hysteretic cycles in ^{137}Cs, ^{238}Pu and $^{239+240}$Pu activity observed at the end of the floods. Indeed, during floods, highly variable contamination by medium to long half-life artificial radionuclides occurs as these are re-introduced in the water flow by the re-uptake of contaminated sediments. The Pu isotope activity ratio in the suspended load, though highly variable (from 0.03 to 0.3), generally shows rising values during floods. This is also a sign of the remobilization of sediments contaminated by industrial inputs (Rolland 2006). The aforementioned data are comparable to the chronology estimated at site PI (Provansal et al. 2010).

Relationship between depositional conditions and the efficiency of radionuclide trapping

Particle grain size is a key parameter for controlling the concentrations of trace metals and radionuclides (Detriché et al. 2010): the finest particles are generally enriched in trace elements due to their larger exchange surfaces. The highest radionuclide concentrations were found in site BA, characterized by the finest silty sediments. Therefore, the low clay content in the fluvial sediment could explain the weaker radionuclide activity compared to measurements in the washload during the "peak" of liquid effluent releases (up to 350 ± 210 Bq kg^{-1} in 1984–1991 at Arles Thomas 1997).

The variation over the last decades in artificial radionuclide source terms complicates the correlations between radionuclide concentrations and grain size because activity levels within sedimentary archives are predominantly governed by the activity of the source term at the time of deposit. The coarser deposits with low exchange surfaces—found mostly at the top of the high banks—are therefore less likely to have high radionuclide concentrations and storages. However, they also belong to a period when Marcoule waste output was already low.

Flood events increase the solid flux—i.e. the sedimentation rate—and the grain size of the deposits: sandy-silts or even fine and coarser sands, were predominant in the deposits from the major Mediterranean floods of recent decades. The grain size and thickness of the flood deposits also depend on the relationships between stream power, channel capacity and bank height. On the lower banks and in the former channels (sites FO, BA and RA), the sediments were deposited by low and moderate river fluxes, with mostly fine particles (clayey-silt or silt), except for the major floods of the last decade. On the high banks (sites PI, MT and MA), vertical accretion only occurs during bankfull discharge of the major floods. Since the crests of the embankments have grown higher during the twentieth Century and the channel bottom has become deeper, the "effective bankfull discharge" automatically increases with time and the sedimentary record becomes discontinuous (Moody and Troutman 2000). The erosion of banks upstream of the study site can complicate the use of radionuclides as chronological markers, as illustrated by the presence of a large mass of reworked organic matter in the flood deposit of November 1993, characterized by high ^{137}Cs activity (Provansal et al. 2010).

Thus, although bank topography and grain size may have a role in inducing differences in the storage of contaminants, they do not suffice to explain why the high PI banks and the low FO banks are contaminated by artificial radionuclides released by nuclear industrial activities, while the high MA and MT banks show very low contamination. Other factors need to be considered.

Relationship between post-depositional conditions and the efficiency of radionuclide trapping

Radionuclide activity may be affected by vertical migration processes, depending on grain-size heterogeneity within the sedimentary profiles (Walling and He 1997), the bank height, pH and redox conditions, the amount and type of organic material, the biological activities and time. These also include hydro-geochemical factors such as the possible desorption of particle-reactive contaminants towards connecting floodplain aquifers, leading either to vertical migration processes or to diffusive exchanges towards groundwater in the case of regularly or permanently submerged systems (such as the former channels).

Nevertheless, the long-term trapping is unaffected by such migration processes along the PI, FO and BA sedimentary profiles, where radionuclides trapping is consistent with the history of bank sedimentation, determined using either naturally occurring radionuclides ($^{210}Pb_{xs}$), flux history or/and differential topo-bathymetric surveys by GIS (Provansal et al. 2010; Ferrand et al. 2012). In contrast to the other sites, the former RA channel is permanently connected to Rhône River groundwater. The absence of higher ^{137}Cs activity levels with depth could suggest high sedimentation rates. Indeed, according to the observations made by Detriché et al. (2010) within the Loire river sandy system, such a monotonous profile ^{137}Cs value corresponds to a high accretion rate enhanced by woody vegetation causing high flow resistance and sediment trapping. Nevertheless, profiles observed in these particularly dynamic water-saturated fine grained porous media could also be linked to a continuous and progressive desorption of ^{137}Cs from contaminated deposited particles towards the soluble phase, until equilibrium with the Rhône waters. Further experiments consisting, for example, in long core sampling in such humid environments are required to buttress this hypothesis. The storage processes only affect medium to long half-life radionuclides, such as ^{137}Cs, ^{241}Am and plutonium isotopes. Radionuclides with shorter half-lives, such as ^{60}Co (5.3 year), were not detected in the samples even though they were released into river waters in concentrations somewhat similar to those of ^{137}Cs. Finally, concentrations and storage of radionuclides within alluvial margins depend on the element's specific radioactive decay period, as short half-life radionuclides disappear through disintegration (Lauer and Willenbring 2010).

Relationship between radionuclide concentration, river geomorphic evolution and industrial activity

An important factor in radionuclide enrichment is relative upstream or downstream location along the Rhône River. Sites MT and MA, located on the two deltaic branches, contain negligible values of ^{137}Cs (<10 Bq kg^{-1}) and Pu isotopes, and ^{241}Am values under detection limits, while the three upstream sites (PI, FO, and BA) display higher concentrations. The various times of fluvial metamorphosis, earlier in the delta, later upstream (Antonelli et al. 2004; Bravard 2010) generate the heterogeneous chronology in geomorphic evolution (bank accretion, channel bed erosion and potential flooding on the banks), as depicted in Fig. 3.

Downstream of the deltaic bifurcation, metamorphosis began at the end of the nineteenth Century as a result of the low slope and the sandy mobile bedload. At site MT (Fig. 5), the braided fluvial system became a straight sinuous channel, limited by high banks since the beginning of the twentieth Century. The vertical variations in grain size correlate with the changes in bank construction. The early vertical accretion drastically reduced overflow at the top of the riverbank, thus explaining the lack of radionuclides below a depth of 40 cm; in the upper part, the low ^{137}Cs concentrations and AR Pu values (Table 1) are characteristic of the deposits resulting from the major floods of the last decade, mainly the 2003 Q_{100} flood. At site MA, the lack of radionuclides below 80 cm could also be explained by the age of the deposits, as they predate the beginning of operations at the Marcoule Plant. However, the small "peak" found at a depth of 40 cm could have been deposited after 1997.

Upstream of the deltaic bifurcation, the persistence of an energetic slope, associated with the inherited gravel bedload, delayed the evolution of the fluvial system (Fig. 4). A high sedimentation rate prevailed during the second part of the twentieth Century at sites PI, FO and BA (Fig. 9). During the last decade, this high rate has been enhanced by the solid flux of several recent strong Mediterranean floods. The deposits can thus clearly record variations in ^{137}Cs, ^{241}Am or Pu isotopes inputs over the last 50 years. The high ^{137}Cs concentrations in the middle part and lower levels of the upper part highlight the activity of the Marcoule Plant until and after 1990. The AR Pu values measured in sites PI and BA (Table 1) record solid flux derived from upstream bank erosion (Provansal et al. 2010; Detriché et al. 2010). In site PI, the strong vertical accretion (13 cm year^{-1} in 1972–1990, 30 cm year^{-1} since 1997) was enhanced by the geomorphic context (dense riparian forest, lower hydraulic energy at the entrance to a former branch, protection provided by two groynes), despite a deepening (4.5 m since 1870, Fig. 9) of the main channel. Sites FO and BA are regularly submerged by moderate floods due to the low altitude of the bank and the moderate channel incision (3 m since 1870, Fig. 9). The lower vertical sedimentation rate (6–7 cm year^{-1}) can be explained by the presence of the large flat alluvial margin (site FO) or by the vertical space created by navigation locks (site BA).

The chronology of deposits, determined by the chronology of fluvial "metamorphosis," seems to be an important factor responsible for the variability of contaminants in Rhône riverbank sediments, in association with grain size or bank topography. The combination of the timing of three main factors (channel deepening/narrowing, chronology of major floods exceeding the bankfull discharge and chronology of contaminant nuclear flux) determines the importance and the spatial distribution of contamination. In the deltaic branches, the early fluvial channel deepening and fluvial "metamorphosis" did not result in sedimentation at the top of the banks during the weaker floods of the 1950–1990 period, when the Marcoule

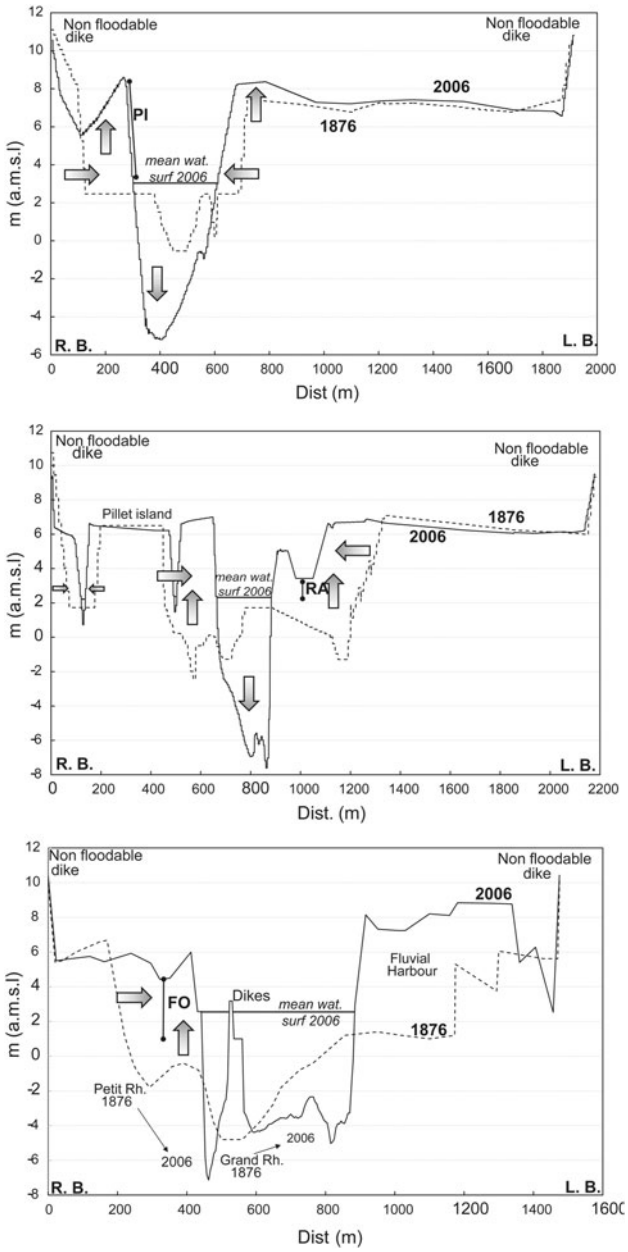

Fig. 9 Evolution of the channel cross-sections in front of the sites PI, RA and FO. The *arrows* indicate the geomorphic evolution (vertical/lateral accretion, erosion in the channel bed)

spent-fuel reprocessing plant was active. In contrast, sites located upstream of the deltaic embranchment, which were later modified by the changes in channel dynamics, efficiently trapped the contaminated sediment over the same period. High sedimentation rates in the upstream sites during the last decade allow for higher radionuclide concentrations, though levels are still influenced by the grain-size and the local morphology (low/high banks, entry of a former branch, artificial trap created by navigation locks). Only the groundwater context of site RA caused a decrease in ^{137}Cs concentrations. During the last decade (1993–2003), major floods inundated all the sites, but the resulting deposits are not highly contaminated by radionuclides, as a result of lowered output from the Marcoule spent-fuel reprocessing plant.

What is the significance of our results for the river as a whole? What are the implications for river management?

The study sites show high spatial variations in radionuclide storage. Several GIS models (Maillet et al. 2007; Raccasi 2008) allowed cautious extrapolations used to quantify or evaluate the volume of sediment trapped in the banks and alluvial margins. Since 1950, the estimated accumulation reached 1.48×10^6 tons along the Grand Rhône (main deltaic branch) and is negligible along the Petit Rhône. Upstream, the global storage in the PI, FO and RA areas is 12.8×10^6 tons. The erosion of sediment and contaminants and their subsequent release into the water system could pose a serious risk and affect the Mediterranean trophic chain. However, the radionuclide levels measured in Arles during floods (Antonelli et al. 2008) do not currently show a significant increase compared to the inputs from the drainage basin. The weak erosion of the banks explains the low rate of remobilized radionuclides. The infrastructure and the plant cover protect contaminated sites, even though the exact length of time of storage is hard to determine. Still, knowledge of these storage areas has important implications for river management because flood abatement measures recommend the implementation of improved flow and discharge conditions involving the remobilization of sediments locked up in the alluvial margins, particularly in the former barred channels and in the compartments. It is therefore essential to identify the factors affecting contaminant concentrations and to establish the specific impacts of the various fluvial practices on the sedimentation rate.

Conclusion

Artificial radionuclide concentrations in alluvial banks of the lower Rhône River exhibit high spatial variability. Within the six study alluvial margin systems, three demonstrated a clear retention of particle-reactive trace contaminants that have been introduced into the river since the middle of twentieth Century.

The correlation between concentration levels and sedimentation rates is not a systematic one, as the highest sedimentation rates (after 1990) correspond to lower contaminant levels. Grain size variations and bank topography play an important role: fine sediment trapped in low-bank areas (sites FO and BA) show the highest concentrations, as do some silty-clay beds in the high banks (site PI).

However, within several water-saturated areas, such as site RA in a former branch, stored fine sediment shows low levels of contamination that could be due to partial desorption of contaminants towards the soluble and mobile phase in the course of drainage by the alluvial aquifer. The complex relationship between the timelines of the following factors seems to provide also a good explanation for the spatial diversity within the concentrations: the fluvial "metamorphosis," the Rhône flood discharge history and the nuclear outputs from the Marcoule Plant. The chronology of the river "metamorphosis," which has conditioned the banks' sedimentary accretion throughout the twentieth century, was itself affected by the construction of river engineering works and the system's geomorphic response to these installations. The response was different upstream and downstream of the delta bifurcation, depending on the energy of the slope and the nature of the bedload. Sediment deposition on the top of the banks is also a function of the spatial variability of channel incision, which controls bankfull discharge (Q_{bf} values). Finally, the highest flows (the ones capable of increasing the sedimentation rate) did not occur at the same time as the nuclear waste releases.

Recommendations regarding the rehabilitation of the riverbanks should therefore be guided by prior studies of the history and geomorphic evolution of these banks. Proper recommendations require that the different types of storage systems be extrapolated for the entire river system. The building of GIS models and the measures of the current bank erosion conditions allow us to construct an outline for this purpose.

Acknowledgments The authors acknowledge the research of several Masters students on the geomorphic evolution of the lower Rhône River. Thanks to P. Pentsch (Provence University) for his help with the figures, and to A. Champelovier, P. Paulat and D. Mourier for their excellent fieldwork. This work received support from the French National Research Agency (ANR) through the ANR-EXTREMA project (contract # ANR-06-VULN-005, 2007–2010, «Vulnérabilité, milieux et climat») and from the "Mer PACA" and "Gestion des Risques et Vulnérabilité des territories" business and research clusters. Liquid discharge values in Arles were made available thanks to the CNR (Compagnie Nationale du Rhône).

References

Aalto R, WE Dietrich (2005) Sediment accumulation determined with ^{210}Pb geochronology for Strickland River flood plains, Papua New Guinea. International Association of Hydrological Sciences Publication, Wallingford

Aalto R, Lauer JW, Dietrich WE (2008) Spatial and temporal dynamics of sediment accumulation and exchange along Strickland River floodplains (Papua New Guinea) over decadal-to-centennial timescales. J Geophys Res 113(F1):F01S04

Alekseevsky NI, Berkovich KM, Chalov RS (2008) Erosion, sediment transportation and accumulation in rivers. Int J Sediment Res 23:93–105

Antonelli C (2002) Flux sédimentaires et morphogenèse récente dans le chenal du Rhône aval. Dissertation, Aix-Marseille University

Antonelli C, Provansal M, Vella C (2004) Recent morphological changes of a channel in a deltaïc environment, the case of the Rhône River, France. Geomorphology 57:385–402

Antonelli C, Eyrolle F, Rolland B, Provansal M, Sabatier F (2008) Suspended sediment and ^{137}Cs fluxes during the exceptional December 2003 flood in the Rhone River, Southeast France. Geomorphology 95:350–360

Appleby PG, Nolan PJ, Oldfield F, Richardson N, Higgitt SR (1988) Pb-210 dating of lake sediments and ombrotrophic peats by gamma assay. Sci Total Environ 69:157–177

Arnaud-Fassetta G (2003) River channel changes in the Rhône Delta (France) since the end of the Little Ice Age; geomorphological adjustment to hydroclimatic change and natural resource management. Catena 51:141–172

Bouisset P, Calmet D (1997) Hyper pure gamma-ray spectrometry applied to low-level environmental sample measurements. In: Proceedings of the workshop on the status of measurement techniques for the Identification of nuclear signatures, Geel, Belgium, 1997, ESARDA Report EUR 17312, 1997, p 73

Bouisset P, Lefevre O, Cagnat X, Kerlau G, Ugron A, Calmet D (1999) Direct gamma-X spectrometry measurement of 129I in environmental samples using experimental self-absorption corrections. Nucl Instrum Methods Phys Res 437:114–127

Bravard JP (2010) Discontinuities in braided patterns:the River Rhône from Geneva to the Camargue delta before river training. Geomorphology 117:219–233

Ciszewski D, Turner J (2009) Storage of sediment-associated heavy metals along the channelized Odra River, Poland. Earth Surf Process Landf 34(4):558–572

Ciszewski D, Czajka A, Błażej S (2008) Rapid migration of heavy metals and ^{137}Cs in alluvial sediments, Upper Odra River valley, Poland. Environ Geol 55(7):1577–1586

Collins AL, Walling DE, Leeks GJL (1997) Use of the geochemical record preserved in floodplain deposits to reconstruct recent changes in river basin sediment sources. Geomorphology 19:151–167

Detriché S, Rodriguez S, Macaire JJ, Bonté Ph, Bréhéret JG, Bakyono JP, Jugé Ph (2010) Caesium 137 in sandy sediments of the River Loire (France):assessment of an alluvial island evolving over the last 50 years. Geomorphology 115:11–22

Duffa C, Renaud P (2005) ^{238}Pu and $^{239+240}$Pu inventory and distribution through the lower Rhone valley terrestrial environment (Southern France). Sci Total Environ 348:164–172

Eyrolle F, Charmasson S, Louvat D (2004) Plutonium isotopes in the lower reaches of the river Rhône over the period 1945–2000: fluxes towards the Mediterranean Sea and sedimentary inventories. J Environ Radioactiv 74 (Special issue): 127–138

Eyrolle F, Louvat D, Métivier JM, Rolland B (2005) Origins and levels of artificial radionuclides within the Rhône River waters (France) for the last forty years: towards an evaluation of the radioecological sensitivy of river systems. Radioprotection 40:435–446

Eyrolle F, Duffa C, Antonelli C, Rolland B, Leprieur F (2006) Radiological consequences of the extreme flooding on the lower course of the Rhone valley (December 2003, South East France). Sci Total Environ 366:427–438

Eyrolle F, Provansal M, Villiet J, Raccasi G, Radakovitch O, Gurriaran R, Antonelli C (2008a) Evidence for delayed source of long lived artificial radionuclides from a managed river banks (Rhône River, Southern France). In: Proceedings of the 11th international symposium on the interactions between sediments and water, Esperance, Australia, 17–22 Feb 2008

Eyrolle F, Claval D, Gontier G, Antonelli C (2008b) Radioactivity levels in major French rivers: summary of monitoring chronicles

acquired over the past thirty years and current status. J Environ Monit 10:800–811

Ferrand E, Eyrolle F, Radakovitch O, Provansal M, Dufour S, Vella C, Raccasi G, Gurriaran R (2012) Heavy metals and artificial radionuclides records in riverbanks sediments of the lower Rhône River (South-East France). Geochimica Cosmochimica Acta, Special issue Environmental Records of Anthropogenic Impacts 82:163–182

Forsberg S, Rosén K, Fernandez V, Juhan H (2000) Migration of ^{137}Cs and ^{90}Sr in undisturbed soil profiles under controlled and close-to-real conditions. J Environ Radioact 50(3):235–252

Gee GW, Bauder JW (1986) Particle-size analysis. In: Klute A (ed) Methods of soil analysis. Madison, WI

Goutelard F, Morello M, Calmet D (1998) Alpha spectrometry measurement of Am and Cm at trace levels in environmental samples using extraction chromatography. J Alloys Compd 271–273:25–30

He Q, Walling DE (1996) Use of fallout Pb-210 measurements to investigate long term rates and patterns of overbank sediment deposition on floodplains of lowland rivers. Earth Surf Proc Land 21:141–154

Hochella MF, White AF (1990) Mineral–water interface geochemistry. In: Hochella MF Jr, White AF (eds) Review in mineralogy, vol 23. Mineralogical Society of America, Washington DC, p 663

Kiss T, Fiala K, Sipos G (2008) Alterations of channel parameters in response to river regulation works since 1840 on the Lower Tisza River (Hungary). Geomorphology 98:96–110

Lauer JW, Willenbring J (2010) Steady state reach-scale theory for radioactive tracer concentration in a simple channel/floodplain system. J Geophys Res 115(F4):F04018

Maillet G, Raccasi G, Provansal M, Sabatier F, Antonelli C, Vella C, Fleury J (2007) Transferts sédimentaires dans le bas Rhône depuis le milieu du XIXème siècle, essai de quantification. Geographie physique et Quaternaire 61:37–50

Middelkoop H (2000) Heavy-metal pollution of the river Rhine and Meuse floodplains in the Netherlands. Neth J Geosci 79:411–428

Miralles J, Radakovitch O, Cochran JK, Véron A, Masqué P (2004) Multitracer study of anthropogenic contamination records in the Camargue, Southern France. Sci Total Environ 320(1):63–72

Miralles J, Arnaud M, Radakovitch O, Marion C, Cagnat X (2006) Radionuclide deposition in the Rhône River Prodelta (NW Mediterranean sea) in response to the December 2003 extreme flood. Mar Geol 234:179–189

Moody JA, Troutman BM (2000) Quantitative model of the growth of floodplains by vertical accretion. Earth Surf Proc Land 25:115–133

Piégay H, Hupp CR, Citterio A, Dufour S, Moulin B, Walling DE (2008) Spatial and temporal variability in sedimentation rates associated with cutoff channel infill deposits: Ain River, France. Water Resour Res 44:W05420

Pont D, Simonnet JP, Walter AV (2002) Medium-term changes in suspended sediment delivery to the ocean: consequences of catchment heterogeneity and river management (Rhône river, France). Estuar Coast et Shelf Sci 54:1–18

Provansal M, Villiet J, Eyrolle F, Raccasi G, Gurriaran R, Antonelli C (2010) High-resolution evaluation of recent bank accretion rate of the managed Rhone: a case study by multi-proxy approach. Geomorphology 117:287–297

Raccasi G (2008) Mutations morphologiques récentes du Rhône aval, recherches en vue de la restauration hydraulique et de la gestion des crues. Dissertation, Aix-Marseille University

Reineck HE, Singh IB (1980) Depositional sedimentary environments, 2nd edn. Springer Verlag, Berlin

Rolland B (2006) Transfert des radionucléides artificiels par voie fluviale: conséquences sur les stocks sédimentaires rhodaniens et les exports vers la Méditerranée. Dissertation, Aix-Marseille University

Rolland B, Eyrolle F, Bourles D (2004) Removal of sedimentary stocks and associated radioactivity in the lower Rhône river (South Eastern France), Proceedings of the International Conference on isotopes in Environmental Studies—Aquatic Forum, Monte-Carlo, Monaco, 25–29 October 2004: 301–302

Steiger J, Gurnell AM, Ergenzinger P, Snelder D (2003) Sedimentation in the riparian zone of an incising river. Earth Surf Process Landf 26:91–108

Surian N, Rinaldi M (2003) Morphological response to river engineering and management in alluvial channels in Italy. Geomorphology 50:307–326

Thomas AJ (1997) Input of artificial radionuclides to the Gulf of Lions and tracing the Rhône influence in marine surface sediments. Deep-Sea Res II 44:577–595

Walling DE, He Q (1997) Use of fallout ^{137}Cs in investigations of overbank sediment deposition on river floodplains. Catena 29:263–282

Walling DE, He Q (1998) The spatial variability of overbank sedimentation on river floodplains. Geomorphology 24:209–223